International Journal of Science & Advanced Technology
ISSN: 3083-9335

Performance and Emission Analysis of Diesel-Turpentine Blends in a Compression Ignition Engine

Syazwana Sapee[1], Ahmad Fitri Yusop[1], Asep Kadarohman[2], Fitri Khoerunnisa[2], Erdiwansyah[3,4]

[1]Faculty of Mechanical and Automotive Engineering Technology, Universiti Malaysia Pahang Al Sultan Abdullah, 26600, Malaysia
[2]Department of Chemistry, Faculty of Mathematics and Science, Indonesia University of Education, Indonesia
[3]Department of Natural Resources and Environmental Management, Universitas Serambi Mekkah, Banda Aceh, 23245, Indonesia
[4]Centre for Automotive Engineering, Universiti Malaysia Pahang Al Sultan Abdullah, Malaysia

Corresponding Author: syazwana.sapee@gmail.com

Abstract

This study investigates the effects of diesel blended with turpentine oil and oxygenated additives namely turpentine–diesel, oxygenated turpentine–diesel) alpha-pinene–diesel, and oxygenated alpha-pinene–diesel on engine performance, combustion characteristics, and emissions in a single-cylinder compression ignition engine under various speeds and loads. The in-cylinder pressure (ICP) analysis reveals that all blended fuels showed higher maximum ICP values than diesel, ranging from 76 bar to 79 bar compared to 75 bar for diesel, an improvement of approximately 1.6% to 5.3%. The heat release rate (HRR) analysis indicates that additive blends enhanced combustion, with maximum HRR reaching 73 J/°CA for TD, compared to 68 J/°CA for diesel, which is an increase of up to 7.3%. CO_2 emissions for additive blends were slightly higher than D, with OAPD reaching up to 0.6% compared to 0.21% for diesel. Carbon monoxide emissions showed minimal differences, with peak values between 0.043% and 0.046% across all fuels. Notably, NO_x emissions significantly increased, with APD reaching 230 ppm compared to 220 ppm for D, reflecting an increase of up to 50%. The ANOVA results confirm that engine speed and load are statistically significant parameters ($p < 0.0001$) affecting combustion and emissions. The study concludes that additive-diesel blends enhance engine performance metrics such as ICP and HRR but with trade-offs in NO_x emissions due to intensified premixed combustion.

Article Info
Received: 12 April 2025
Revised: 10 May 2025
Accepted: 15 May 2025
Available online: 15 May 2025

Keywords
Additive diesel blends
In-cylinder pressure
Heat release rate
Engine emissions
Compression ignition engine

1. Introduction

The growing global concern over fossil fuel depletion and environmental degradation has prompted significant interest in alternative fuels for internal combustion engines. Among these, renewable and biodegradable fuel additives derived from natural sources have gained increasing attention. Diesel engines, known for their efficiency and durability, are widely used in transportation and power generation. Still, they contribute substantially to emissions of nitrogen oxides (NO_x), carbon monoxide (CO), carbon dioxide (CO_2), and unburned hydrocarbons (HC) (Elkelawy, Draz, Antar, & Seleem,

2025; Ghazali, Rosdi, Erdiwansyah, & Mamat, 2025; Muhibbuddin, Muchlis, Syarif, & Jalaludin, 2025; S. M. Rosdi, Maghfirah, Erdiwansyah, Syafrizal, & Muhibbuddin, 2025). Therefore, exploring alternative fuel strategies that enhance combustion efficiency while reducing emissions is a vital research direction. Several studies have investigated the impact of blending diesel with bio-derived additives to improve performance and reduce emissions. Turpentine oil, obtained from pine resin, has emerged as a potential additive due to its high volatility, lower viscosity, and favourable combustion characteristics (Chivu et al., 2023; Muhibbuddin, Hamidi, & Fitriyana, 2025; Nizar, Yana, Bahagia, & Yusop, 2025; S. M. M. Rosdi, Erdiwansyah, Ghazali, & Mamat, 2025). Turpentine facilitates better atomization and mixing when blended with diesel, improving premixed combustion. Oxygenated fuels improve combustion efficiency by increasing oxygen availability in the combustion chamber, which can lead to more complete combustion (Alenezi, Erdiwansyah, Mamat, Norkhizan, & Najafi, 2020; Fitriyana, Rusiyanto, & Maawa, 2025; Li et al., 2024; S. M. Rosdi, Ghazali, & Yusop, 2025).

The use of oxygenated bio-additives tends to increase the heat release rate (HRR) in the premixed phase, enhancing thermal efficiency (Alenezi et al., 2021; Muchlis, Efriyo, Rosdi, & Syarif, 2025; Muzakki & Putro, 2025; Saha, Sinha, & Roy, 2021). However, this may also lead to increased in-cylinder pressure (ICP) and peak temperatures, which are known to elevate NO_x emissions through the thermal Zeldovich mechanism. Increasing the proportion of oxygenated components can affect injection timing and combustion phases, thereby altering emission characteristics (Ganapathy, Gakkhar, & Murugesan, 2011; Gani et al., 2025; Iqbal, Rosdi, Muhtadin, Erdiwansyah, & Faisal, 2025; Mohan, Yang, & kiang Chou, 2013). In addition, fuel blends with higher volatility and lower cetane numbers could increase ignition delay (ID), allowing for more significant fuel accumulation before combustion and consequently producing a more intense HRR during the premixed phase (Irhamni, Kurnianingtyas, Muhtadin, Bahagia, & Yusop, 2025; Jalaludin, Kamarulzaman, Sudrajad, Rosdi, & Erdiwansyah, 2025; Molina, Garcia, Monsalve-Serrano, & Villalta, 2021; Muhtadin, Rosdi, Faisal, Erdiwansyah, & Mahyudin, 2025). While beneficial for combustion efficiency, this phenomenon must be carefully balanced against the potential rise in pollutant formation, particularly NO_x and CO_2. Hence, additives like alpha-pinene and other turpentine derivatives need comprehensive evaluation under varying engine conditions.

Despite the promising potential of additive-diesel blends, there remains a gap in understanding their full impact under different engine speeds and loads. Few studies have systematically analyzed the interaction effects between engine parameters and additive type on ICP, HRR, and gaseous emissions using advanced statistical tools such as ANOVA and response surface methodology. Moreover, the quantitative influence of each factor and their quadratic interactions are rarely compared in a unified experimental framework. Therefore, this study aims to comprehensively evaluate the combustion characteristics and emission behaviour of various additive-diesel blends under different operating conditions, namely, TD, OTD, APD, and OAPD. The objective is to determine how engine speed, load, and fuel composition interact to affect key parameters such as ICP, HRR, CO, CO_2, and NO_x emissions. By employing statistical modelling and 3D response surface analysis, this work provides insights into optimizing alternative fuel blends for sustainable engine performance.

2. Methodology

This section outlines the methodology employed to evaluate the performance, combustion behaviour, and exhaust emissions of the test fuels in a diesel engine. It details the experimental engine test setup, including engine specifications, integrated systems, and key equipment. Additionally, it explains the measurement techniques and instruments used for data collection, along with a comprehensive overview of the sensor integration and data acquisition system.

This section covers the experimental engine setup schematic diagram, engine specifications, components, and measurement methods. The engine test rig was set up, as presented in the schematic diagram in **Fig. 1**. The experiment was conducted at the Engine Performance Laboratory, Faculty of Mechanical and Automotive Engineering Technology, Universiti Malaysia Pahang, Pekan, Pahang.

The main component of this experiment is the engine. The engine is a single-cylinder, four-stroke, naturally aspirated, water-cooled diesel engine, direct-injection CI Yanmar TF120M engine. **Table 1** presents detailed specifications of the Yanmar TF120M engine. The engine used is unmodified, with a 17.7 compression ratio. This engine is equipped with an exhaust gas recirculation (EGR) system. However, in this study, the EGR mode is set to off.

The unmodified single-cylinder engine is chosen for this study due to its simplicity and ease of operation. Furthermore, engine performance can be investigated more precisely because all the parameters that determine engine power depend on the combustion in a single combustion chamber. A pressure sensor is used to measure the performance characteristics in the engine combustion chamber. Besides, Yanmar TF120M is a water-cooled engine with a cooling system designed to the engine's specific features. The engine is connected to a hydraulic dynamometer with a load controller, as shown in **Fig. 2**.

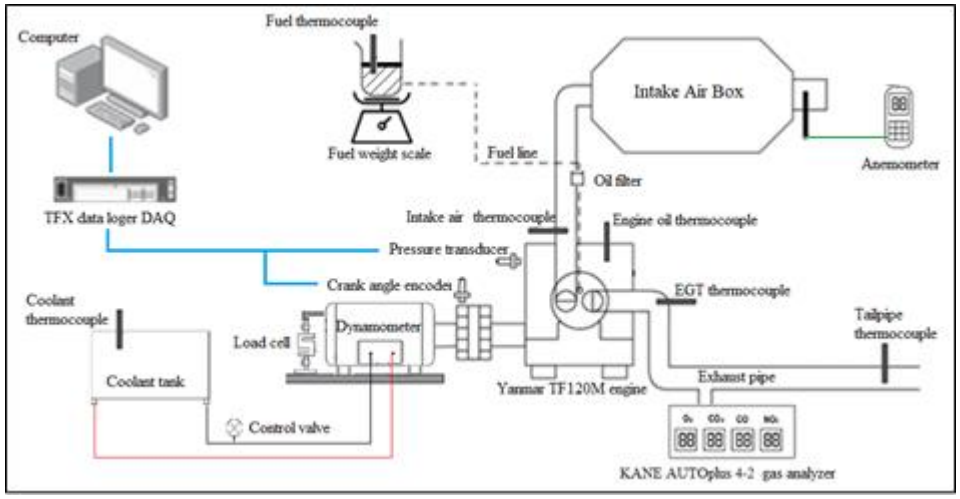

Fig. 1. Schematic diagram of diesel engine test setup

Table 1 presents the technical specifications of the YANMAR TF120M diesel engine, a horizontal, four-stroke, single-cylinder engine with a direct injection system. This engine was manufactured in 2016 and has a cylinder diameter (bore) of 92 mm and a piston stroke (stroke) of 96 mm, with a total cylinder volume of 0.638 litres. This engine can produce a continuous power of 7.82 kW and a maximum power of 8.94 kW at a speed of 2,400 rpm. The maximum torque that can be produced reaches 43.35 N m at 1,800 rpm, indicating that this engine is efficient enough for medium-load applications. Furthermore, this engine has a combustion efficiency indicated by a specific fuel consumption of 169 grams per horsepower-hour (gr/hp.h). The fuel injection time is set at 17° before TDC (Top Dead Center), and the engine has a high compression ratio of 17.7, indicating good thermal efficiency. The cooling system uses water, and the engine is started manually. This engine also uses a naturally aspirated system without a turbo, with the PTO (Power Take-Off) position on the flywheel side, and the crankshaft rotation direction is counterclockwise when viewed from the flywheel. The combination of these specifications makes the YANMAR TF120M suitable for engine performance experiment applications and alternative fuel research.

Table 1. Specification of Yanmar TF120M diesel engine

Description	Specification
Engine model	YANMAR TF120M
Engine year	2016
Engine type	Horizontal, four-cycle, four-stroke, diesel engine
Number of cylinders	1
Continuous power output (kW)	7.82 kW at 2,400 rpm

Description	Specification
Rated power output (kW)	8.94 kW at 2,400 rpm
Bore × Stroke (mm)	92 × 96
Displacement (L)	0.638
Maximum torque (kgf.m/rpm)	43.35 N.m / 1,800 rpm
At 1-hr. rated output (hp/rpm, kW)	12.0 hp / 2,400 rpm (9.0 kW)
Rated continuous output (hp/rpm, kW)	10.5 hp / 2,400 rpm (7.8 kW)
Specific fuel consumption (gr/hp.h)	169 gr/hp.h
Injection timing	17°bTDC
Compression ratio	17.7
Combustion system	Direct injection
Aspiration	Natural aspiration
Cooling system	Water-cooled
Starting system	Manual (hand) starting.
Position of PTO	Flywheel side
The direction of crankshaft rotation	Counterclockwise viewed from the flywheel.

Fig. 2 shows an engine test system with a dynamometer to measure engine performance accurately. In the figure, the engine is connected to a propeller shaft, which is then forwarded to a coupling as a connection to a hydraulic dynamometer. This dynamometer functions to load the engine and measure the power generated. In the system, there is also a control valve that functions to regulate the fluid flow in the dynamometer to control the load and a pressure gauge to monitor the pressure during testing. In addition, a load cell is used to measure the torque the engine generates. These components work in an integrated manner to enable a comprehensive engine performance and efficiency analysis.

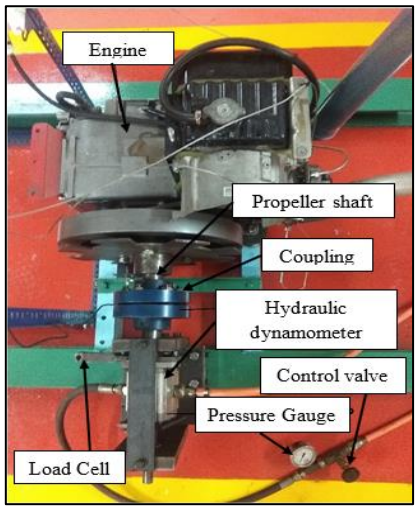

Fig. 2. A dynamometer attached to the engine

3. Result & Discussion

In-cylinder pressure analysis

Table 1 presents the analysis of variance (ANOVA) results for the ICP (In Cylinder Pressure), which helps determine the significance of individual factors and their interactions in the model. The overall model is statistically significant, as indicated by the F-value of 61.53 and a p-value of less than 0.0001. Among the individual variables, A-Speed, B-Load, and C-Fuel exhibit strong significance with p-values < 0.0001, especially B-Load, which has the highest F-value (725.00), implying it is the most influential factor on ICP. Additionally, the quadratic term A^2 is highly significant (F = 134.19), suggesting a non-linear effect of speed on the response.

In contrast, interaction terms AC and BC and the quadratic term B^2 are insignificant, with p-values of 0.1501, 0.2502, and 0.9505, respectively. This indicates that their contribution to the variation in ICP is negligible. The residual value is relatively low (53.73), and the lack of fit value equals the residual, suggesting that the model adequately fits the data without significant unexplained variation. Overall, the results confirm that the model is reliable, with key factors like speed, load, and fuel playing substantial roles in influencing the ICP. This matches with the ICP derivation in **Eq. 1**, which describes the relationship between ICP and engine speed (A), engine load (B), and fuels (C), where C1, C2, C3, C4, and C5 are D, TD, OTD, APD, and OAPD, respectively.

Table 1. Analysis of variance table for ICP

Source	Some of Squares	df	Mean Square	*F*-Value	*p*-Value Prob > *F*	
Model	1,195.78	17	70.34	61.53	<0.0001	significant
A-Speed	88.20	1	88.20	77.15	<0.0001	
B-Load	828.87	1	828.87	725.00	<0.0001	
C-Fuel	62.94	4	15.74	13.76	<0.0001	
AB	22.56	1	22.56	19.73	<0.0001	
AC	8.11	4	2.03	1.77	0.1501	
BC	6.38	4	1.59	1.39	0.2502	
A^2	153.41	1	153.41	134.19	<0.0001	
B^2	4.457E-003	1	4.457E-003	3.899E-003	0.9505	
Residual	53.73	47	1.14			
Lack of Fit	53.73	27	1.99			

Table 2 continues the ANOVA summary and includes additional model performance metrics. The total corrected sum of squares is 1,249.52 with 64 degrees of freedom, reflecting the dataset's total variability. The pure error is reported as zero, indicating that the model perfectly fits the replicated experimental data points, implying a tight model-data agreement. The absence of pure error also emphasizes that the residual variation observed in Table 1 is mainly due to model limitations rather than experimental inconsistency. The statistical quality of the regression model is further demonstrated by the R-squared (0.9570), adjusted R-squared (0.9414), and predicted R-squared (0.9007) values. These values suggest a firm fit between the model and experimental data. The high R-squared indicates that the model explains 95.70% of the total variation in ICP. Meanwhile, the adjusted R-squared corrects for the number of predictors and remains high, showing the model's robustness. The predicted R-squared value, which is slightly lower but still above 0.90, confirms that the model has good predictive ability for new observations, further validating the reliability and effectiveness of the regression model.

Table 2. Continued

Source	Some of Squares	df	Mean Square	F-Value	p-Value Prob > F
Pure Error	0.000	20	0.000		
Cor Total	1,249.52	64			

The R-squared sum of squares 0.9570
Adj R-Squared sum of squares 0.9414
Pred R-Squared sum of squares 0.9007

$$ICP = 70.55 - 1.71A + 5.26B - 1.47C_1 - 0.21C_2 + 1.32C_3 - 0.46C_4 - 1.06AB - 0.30AC_1 + 1.02AC_2 - 0.27AC_3 - 0.38AC_4 - 0.58BC_1 + 0.24BC_2 + 0.55BC_3 - 0.52BC_4 - 3.33A^2 + 0.018B^2 \quad (1)$$

The 3D response surface plots for the quadratic model of the maximum ICP of each fuel at various engine speeds and loads are shown in **Fig. 4** (a–e). The maximum ICP increased as the engine load increased for all fuel mixes, as presented by the contour maps. Additionally, as demonstrated in the 3D plots, the ICP increased and then decreased as the engine speed increased. As shown in **Fig. 4** (a–e), each test fuel's ICP minimum and maximum values varied. **Fig. 4** (a) indicates that for various engine speeds and loads of fuel D, the minimum and maximum ICP values are 60 bar and 75 bar, respectively. **Fig. 4** (b–e) illustrates the minimal ICP for TD, OTD, APD, and OAPD, with a value of 61 bar, while the maximum ICP is between 76 bar and 79 bar. Hence, the improvement of ICP for the test fuels is around 1.6–5.3%, compared to D. Overall, the peak ICP of additive-diesel blends is slightly higher than D under all engine speeds and loads. This is due to the lower viscosity of turpentine oil, which accelerates the mixing of air and fuel, resulting in increased cylinder pressure.

Additionally, turpentine oil has a lower cetane index than diesel; thus, an increase in fuel build-up inside the cylinder leads to higher pressure generation. Oxygenated additives have a higher latent heat of vaporisation than diesel. Park et al. found that increasing the oxygenated additive concentration in blends produced a drop in maximum ICP (Park, Youn, & Lee, 2011). This affected the injection line pressure and initiation, affecting the combustion phases (Alptekin, Canakci, Ozsezen, Turkcan, & Sanli, 2015).

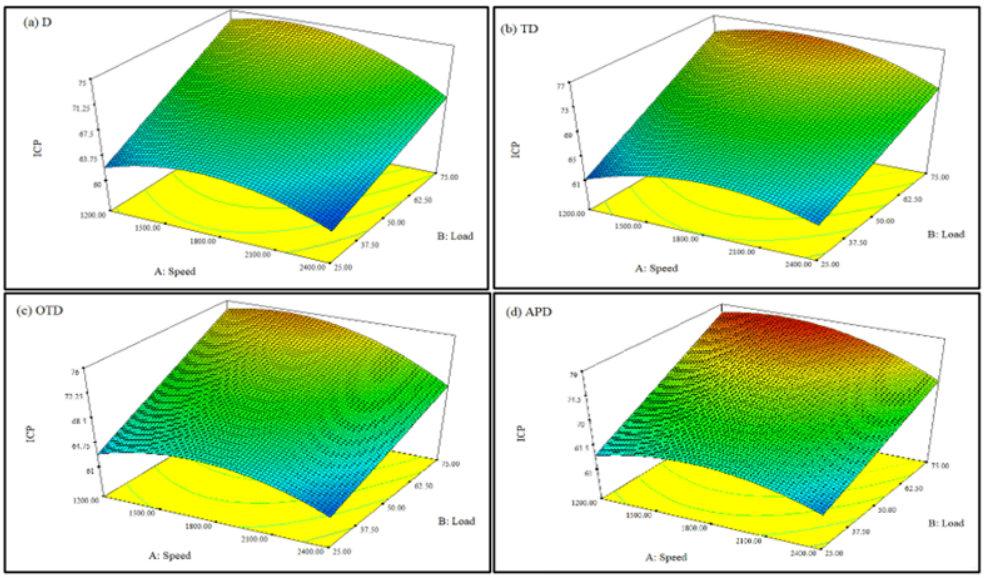

Fig. 4. Response surface plots for ICP variation in test fuels of (a) D, (b) TD, (c) OTD, (d) APD, and (e) OAPD

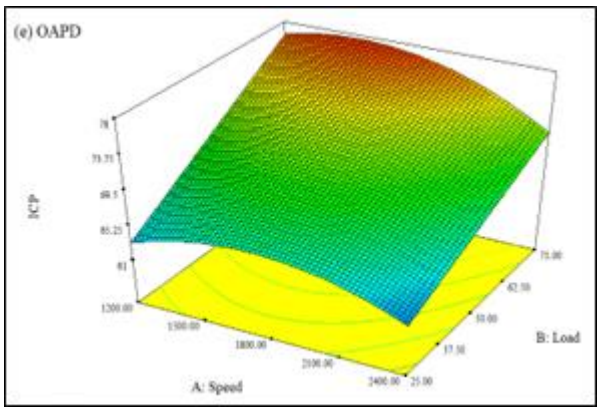

Fig. 5. Continued

Heat release rate analysis

The ANOVA results for HRR at various engine speeds and loads are presented in Table 2. This model has an *F*-value of 12.40 and a *p*-value of less than 0.0001, indicating that the model is significant. The R^2 value is 81.8%, with a difference between the Pred R-squared (60.3%) and the Adj R-squared (75.2%) of less than 0.15. Engine speed and fuels are significant terms in the ANOVA table, whereas engine load has more negligible effects in the sum of squares. This is in line with the HRR in **Eq. 2**. This equation describes the relationship between HRR and engine speed (A), engine load (B), and fuels (C), where C_1, C_2, C_3, C_4, and C_5 are D, TD, OTD, APD, and OAPD, respectively.

$$HRR = 59.36 + 4.08A + 1.06B + 0.25C_1 + 2.35C_2 - 0.72C_3 - 1.53C_4 + 3.56AB + 0.71AC_1 + 2.01AC_2 - 1.13AC_3 - 0.98AC_4 - 0.43BC_1 + 2.51BC_2 - 0.61BC_3 - 0.71BC_4 + 1.94A^2 - 4.22B^2 \quad (2)$$

Table 3. Analysis of variance table for HRR

Source	Sum of Squares	df	Mean Square	*F*-Value	*p*-Value Prob > *F*	
Model	1,237.22	17	72.78	12.40	<0.0001	significant
A-Speed	500.54	1	500.54	85.27	<0.0001	
B-Load	34.01	1	34.01	5.79	0.0201	
C-Fuel	111.76	4	27.94	4.76	0.0026	
AB	253.12	1	253.12	43.12	<0.0001	
AC	42.96	4	10.74	1.83	0.1390	
BC	47.57	4	11.89	2.03	0.1060	
A^2	51.97	1	51.97	8.85	0.0046	
B^2	245.48	1	245.48	41.82	<0.0001	
Residual	275.89	47	5.87			
Lack of Fit	275.89	27	10.22			
Pure Error	0.000	20	0.000			
Cor Total	1,513.11	64				

An R-squared sum of squares 0.8177
Adj R-Squared sum of squares 0.7517
Pred R-Squared sum of squares 0.6031

Fig. 6 (a–e) illustrates the 3D response surface plots for the quadratic model of HRR of each fuel at various engine speeds and loads from the 3D contour maps in **Fig. 6** (a–e), as the engine load increased for all fuel mixtures, the maximum HRR increased. In addition, the HRR increased as the engine speeds increased. **Fig. 6** (a) shows that D's lowest and highest HRR values are 49 J/°CA and 68 J/°CA, respectively, for various engine speeds and loads. Figure 4.26 (b–e) shows that the minimum HRR values for TD, OTD, APD, and OAPD are 53 J/°CA, 49 J/°CA, 50 J/°CA, and 49 J/°CA, respectively. Meanwhile, the maximum HRR values for TD, OTD, APD, and OAPD are 73 J/°CA, 64 J/°CA, 65 J/°CA, and 66 J/°CA, respectively. Overall, compared to D, the improvement in the HRR for the test fuels is approximately 2.1%–7.3%. The HRR for all fuels increased significantly when the engine speed changed from low to high. The higher HRR of test fuel during premixed combustion can be attributed to increased fuel accumulation over the longer ID. As the additives are added to the fuels, the maximum HRR increases. This is due to the additives' longer ignition time. The longer ID of additive-diesel blends leads to a more intense premixed combustion phase, resulting in higher HRRs. The diffusion combustion phase is significantly lower for the test fuels because less fuel is consumed in the latter combustion stage, resulting in increased BTE and performance (Buyukkaya, 2010).

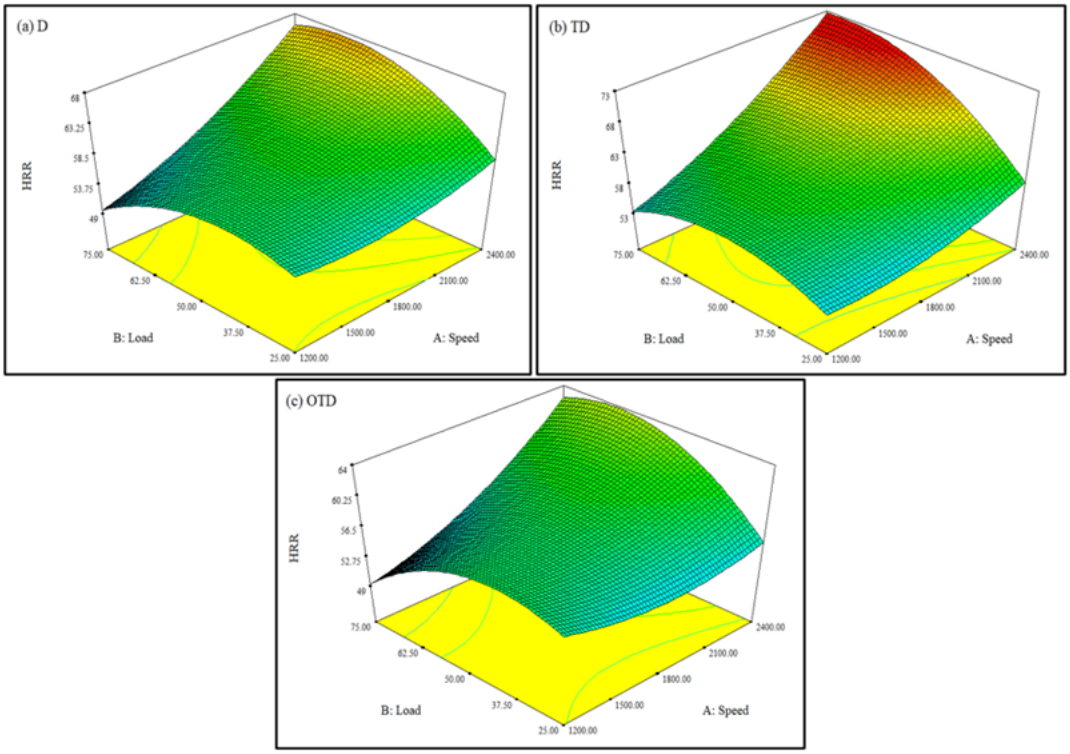

Fig. 6. Response surface plots for HRR variation in test fuels of (a) D, (b) TD, (c) OTD, (d) APD, and (e) OAPD

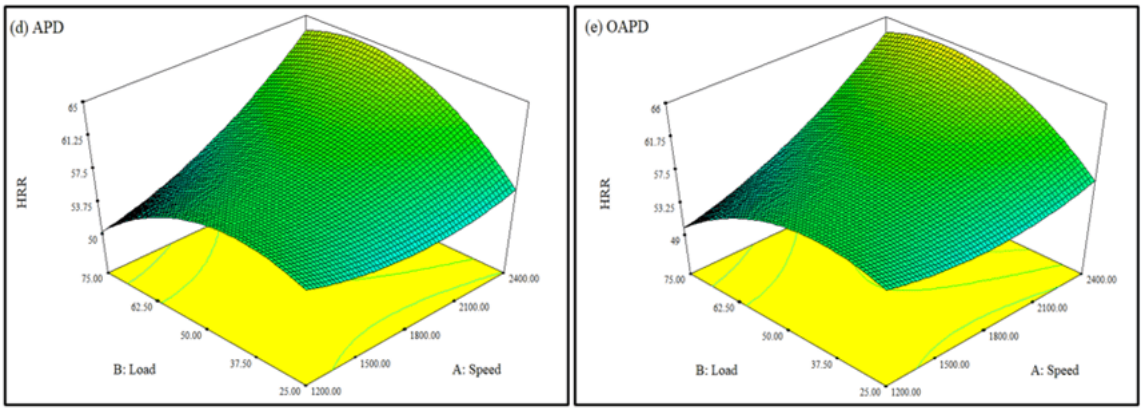

Fig. 7. Continued

Carbon dioxide analysis

The ANOVA results for CO_2 emissions at various engine speeds and loads are shown in **Table 4**. This model has an *F*-value of 73.75. The *p*-value is less than 0.0001; hence, the model is statistically significant. Furthermore, this model's R^2 value is 96.4%. The Pred R-squared and the Adj R-squared have a difference of less than 0.06, 89.3% and 95.1%, respectively. Engine speed is a significant term in the ANOVA table, whereas fuels and engine loads have more negligible effects, as mentioned in the sum of squares. This is similar to the CO_2 equation. **Eq. 3** describes the relationship between CO_2 emissions and engine speed (A), engine load (B), and fuels (C), where C_1, C_2, C_3, C_4, and C_5 represent D, TD, OTD, APD, and OAPD, respectively.

$$CO_2 = 0.76 + 0.74A + 0.050B - 9.231E - 004C_1 + 0.071C_2 - 0.022C_3 + 0.043C_4 - 0.10AB + 0.018AC_1 + 0.10AC_2 - 0.035AC_3 + 0.010AC_4 + 0.028BC_1 + 4.667E - 003BC_2 + 0.19BC_3 - 0.020BC_4 + 0.44A^2 + 0.016B^2 \quad (3)$$

Table 4. Analysis of variance table for CO_2 emissions

Source	Some of Squares	df	Mean Square	*F*-Value	*p*-Value Prob > *F*	
Model	20.93	17	1.23	73.75	<0.0001	significant
A-Speed	16.58	1	16.58	992.93	<0.0001	
B-Load	0.076	1	0.076	4.55	0.0381	
C-Fuel	0.20	4	0.051	3.03	0.0265	
AB	0.22	1	0.22	13.21	0.0007	
AC	0.13	4	0.034	2.01	0.1086	
BC	0.46	4	0.12	6.89	0.0002	
A^2	2.71	1	2.71	162.31	<0.0001	
B^2	3.520E-003	1	3.520E-003	0.21	0.6482	
Residual	0.78	47	0.017			
Lack of Fit	0.76	27	0.028	20.20	<0.0001	significant
Pure Error	0.028	20	1.388E-003			
Cor Total	21.72	64				

An R-squared sum of squares 0.9639
Adj R-Squared sum of squares 0.9508
Pred R-Squared sum of squares 0.8925

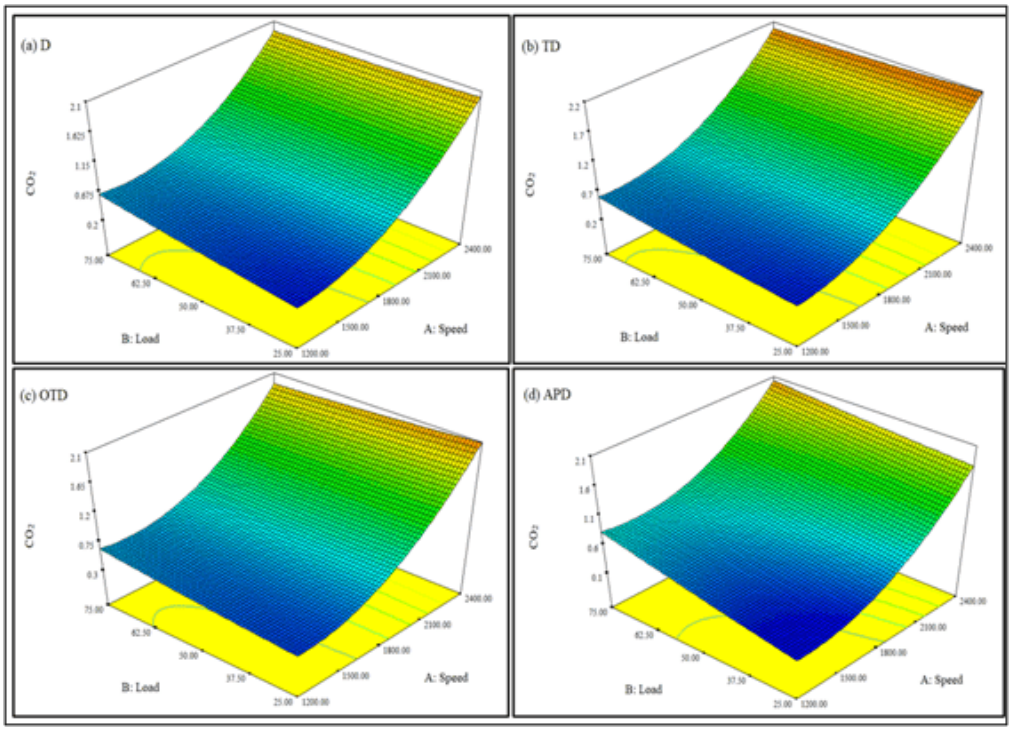

Fig. 8. Response surface plots for CO2 variation in test fuels of (a) D, (b) TD, (c) OTD, (d) APD, and (e) OAPD

The 3D surface plots for the quadratic model of CO_2 emissions for various fuel blends and engine loads are shown in **Fig. 8** (a–e). Carbon dioxide emissions increased as the engine load increased for all fuel

mixes, as presented by the contour maps. Furthermore, as demonstrated in the 3D plots, CO_2 emissions increased as the engine speed increased. Each test fuel's CO_2 minimum and maximum emission values varied. **Fig. 8** (a) indicates that for various engine speeds and loads, the lowest and highest CO_2 emission values for D are 0.2% and 0.21%, respectively. **Fig. 9** (b–e) illustrates the minimum CO_2 emission values for TD, OTD, APD, and OAPD, which are 0.2%, 0.3%, 0.1%, and 0.45%, respectively. Meanwhile, the maximum CO_2 emissions values are 0.6%, 0.65%, 0.8%, and 0.6% for TD, OTD, APD, and OAPD, respectively. Carbon dioxide emissions increased slightly with the inclusion of additives, according to the 3D interactive plots. Turpentine and alpha-pinene have higher heating values than diesel; these additive-diesel mixes use less fuel than pure diesel. The findings of this investigation are similar to other studies (Arpa, Yumrutas, & Alma, 2010; Yumrutaş, Alma, Özcan, & Kaşka, 2008).

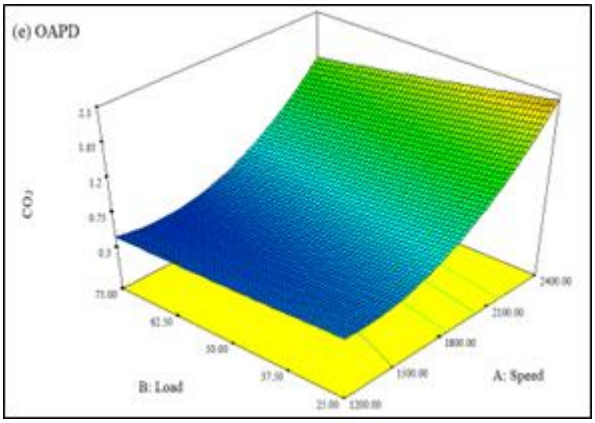

Fig. 9. Continued

Carbon monoxide analysis

Carbon monoxide emissions are produced when there is insufficient O_2 to convert CO to CO_2. This occurs because of incomplete combustion. Equation 4.8 describes the relationship between CO emissions and engine speed (A), engine load (B), and fuels (C), where C_1, C_2, C_3, C_4, and C_5 are D, TD, OTD, APD, and OAPD, respectively. **Table 5** shows the ANOVA findings for CO emissions at different engine speeds and loads. According to the table, the *F*-value for this model is 23.41. The model indicates that it is statistically significant as the *p*-value is less than 0.0001. Moreover, the R^2 value of this model is 89.4%. The difference between the Pred R-squared and the Adj R-squared is less than 0.08, with the Pred R-squared and the Adj R-squared are 78.3% and 85.6%, respectively. The test fuels have lower effects, as stated in the sum of squares, whereas engine speed and load are significant terms in the ANOVA table. This is in line with the given CO emission equation.

$$CO = 0.017 + 0.011A - 2.327E-003B + 6.154E-006C_1 - 1.538E-006C_2 + 6.369E-004\,C_3 - 1.540E-003C_4 - 6.000E-003AB + 4.333E-004AC_1 + 1.000E-003AC_2 - 3.833E-004AC_3 - 6.500E-004AC_4 - 4.567E-004BC_1 + 6.600E-004BC_2 - 1.567E-004BC_3 + 1.100E-004BC_4 + 8.004E-003A^2 + 6.945E-004B^2 \quad (4)$$

Table 5. Analysis of variance table for CO emissions

Source	Some of Squares	df	Mean Square	*F*-Value	*p*-Value Prob > *F*	
Model	5.830E-003	17	3.430E-004	23.41	<0.0001	significant
A-Speed	3.774E-003	1	3.774E-003	257.61	<0.0001	
B-Load	1.624E-004	1	1.624E-004	11.08	0.0017	
C-Fuel	4.660E-005	4	1.165E-005	0.80	0.5344	
AB	7.200E-004	1	7.200E-004	49.14	<0.0001	

AC	1.150E-005	4	2.876E-006	0.20	0.9391	
BC	4.232E-006	4	1.058E-006	0.072	0.9902	
A^2	8.848E-004	1	8.848E-004	60.39	<0.0001	
B^2	6.660E-006	1	6.660E-006	0.45	0.5035	
Residual	6.886E-004	47	1.465E-005			
Lack of Fit	4.886E-004	27	1.810E-005	1.81	0.0875	not significant
Pure Error	2.000E-004	20	1.000E-005			
Cor Total	6.519E-003	64				

An R-squared sum of squares 0.8944
Adj R-Squared sum of squares 0.8562
Pred R-Squared sum of squares 0.7831

The 3D surface plots of the quadratic model for CO emissions for various fuel blends and engine loads are shown in **Fig. 10** (a–e). Carbon monoxide emission increased slightly as the engine load increased for all fuel mixes, as presented by the contour maps. Furthermore, as demonstrated in the 3D plots, CO emissions increased as the engine speed increased. Each test fuel's CO minimum and maximum emission values varied. **Fig. 10** (a) indicates that for various engine speeds and loads, the lowest CO emission of D is 0.01%, and the highest CO emission of D is 0.046%. **Fig. 10** (b–e) illustrates that the lowest CO emission values for TD, OTD, APD, and OAPD are 0.008%, 0.009%, 0.0.11%, and 0.012%, respectively. The highest CO emission values for TD, OTD, and APD are between 0.043% and 0.046%. From the figure, it is notable that the CO emission does not change much between the test fuels. Due to the higher C content of turpentine and oxygenated additives compared to diesel, the combined effect of the previously mentioned variables (low viscosity, high calorific value, and high volatility) is more dominant, resulting in less incomplete combustion of additive-diesel fuels and lower CO emissions. Furthermore, factors that degrade the combustion rate, such as the high latent temperature of turpentine vaporisation, can result in a high oxidation reaction rate of CO, resulting in higher combustion temperature and burning speed, as well as lower CO output (Karikalan & Chandrasekaran, 2016).

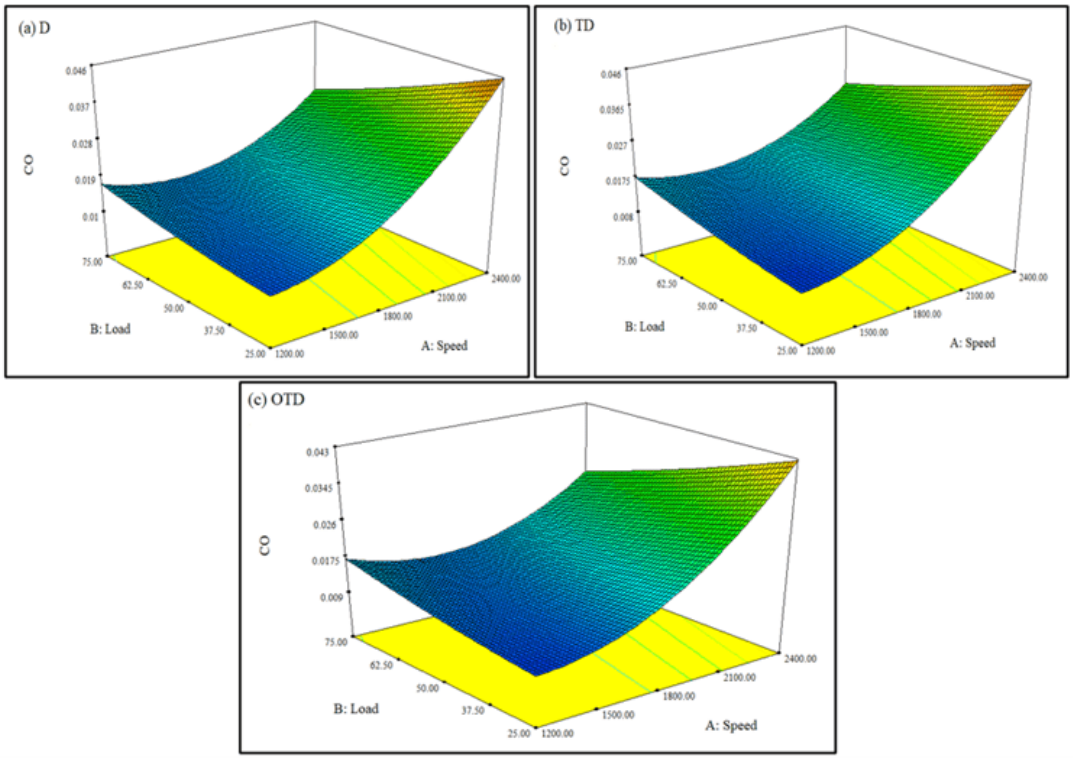

Fig. 10. Response surface plots for CO variation in test fuels of (a) D, (b) TD, (c) OTD, (d) APD, and (e) OAPD

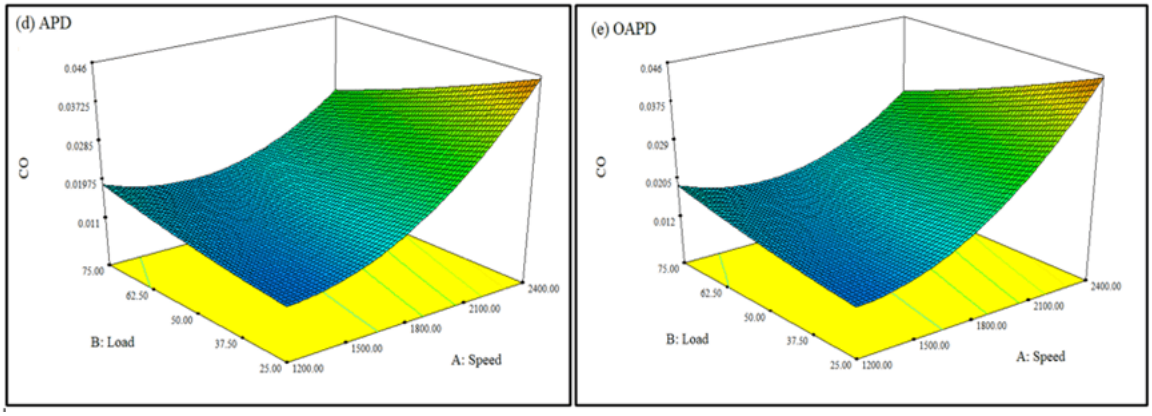

Fig. 11. Continued

Nitrogen oxides analysis

According to the Zeldovich mechanism, NO_X emissions are produced by O_2 concentration, combustion residence time, and combustion temperature. **Table 10** shows the ANOVA findings for NO_X emissions at various engine speeds and loads. The *F*-value for this model is 64.92. The model shows that it is statistically significant because the *p*-value is less than 0.0001. Furthermore, the R^2 value of this model is 95.9%. The difference between the Pred R-squared and the Adj R-squared is less than 0.06%, with the Pred R-squared being 88.9% and the Adj R-squared being 94.4%. The test fuels have more negligible effects in the sum of squares, whereas engine speed and load are significant terms in the ANOVA table. This corresponds to the NO_X emission equation. Equation 4.9 describes the relationship between NO_X emissions and engine speed (A), engine load (B), and fuels (C), where C_1, C_2, C_3, C_4, and C_5 are D, TD, OTD, APD, and OAPD, respectively.

$$NO_X = 84.12 + 55.33A + 34.09B - 0.86C_1 + 3.25C_2 + 4.92C_3 + 1.83C_4 + 7.48AB + 3.06AC_1 + 6.66AC_2 + 6.667E - 003AC_3 - 2.28AC_4 + 2.18BC_1 + 1.46BC_2 + 15.53BC_3 - 3.74BC_4 + 25.37A^2 - 0.038B^2 \quad (5)$$

Table 6. Analysis of variance table for NO_X emissions

Source	Sum of Squares	df	Mean Square	*F*-Value	*p*-Value Prob > *F*	
Model	1.435E+005	17	8,439.82	64.92	<0.0001	significant
A-Speed	91,831.20	1	91,831.20	706.39	<0.0001	
B-Load	34,863.84	1	34,863.84	268.18	<0.0001	
C-Fuel	15,89.59	4	397.40	3.06	0.0255	
AB	1,120.50	1	1,120.50	8.62	0.0051	
AC	685.45	4	171.36	1.32	0.2770	
BC	2,998.88	4	749.72	5.77	0.0007	
A^2	8,890.01	1	8,890.01	68.38	<0.0001	
B^2	0.020	1	0.020	1.501E-004	0.9903	
Residual	6,110.01	47	130.00			
Lack of Fit	6,030.26	27	223.34	56.01	<0.0001	significant
Pure Error	79.75	20	3.99			
Cor Total	1.496E+005	64				

The R-squared sum of squares 0.9592
Adj R-Squared sum of squares 0.9444
Pred R-Squared sum of squares 0.8893

The 3D response surface plots for the quadratic model of NO_X emissions of each fuel at various engine speeds and loads are shown in **Fig. 12** (a–e). **Fig. 12** (a–e) shows a significantly increasing pattern of NO_X emissions corresponding to engine loads and speeds, as illustrated in the 3D surface plots. Each test fuel's NO_X minimum and maximum emission values varied. **Fig. 12** (a) indicates that for various engine speeds and loads, the lowest NO_X emission is 20 ppm, and the highest NO_X emission is 220 ppm for D. **Fig. 12** (b–e) show that the lowest NO_X emission values for TD, OTD, APD, and OAPD are 20 ppm, 30 ppm, 10 ppm, and 40 ppm, respectively. Meanwhile, the highest NO_X emission values for TD, OTD, APD, and OAPD are 220 ppm, 210 ppm, 230 ppm, and 180 ppm, respectively. Compared to the baseline D, these fuels produced higher NO_X emissions in most situations, resulting in a substantial improvement of 18.2–50%. By enhancing premixed combustion due to less slow-burning, adding turpentine and alpha-pinene oil to diesel mixes increases NO_X emissions. Due to turpentine's higher calorific value and lower viscosity, which results in more premixed combustion, higher peak ICP and temperature, and consequently higher NO_X emissions, all test fuel mixes emit more NO_X emissions than diesel fuel. Turpentine has a lower viscosity than diesel; therefore, it has more outstanding atomisation, more air entrainment, and higher fuel-air mixing rates during the premixed combustion phase, resulting in more heat release. This results in higher premixed combustion rates, peak ICPs, and temperatures, all contributing to increased NO_X emissions (Agarwal, 2007).

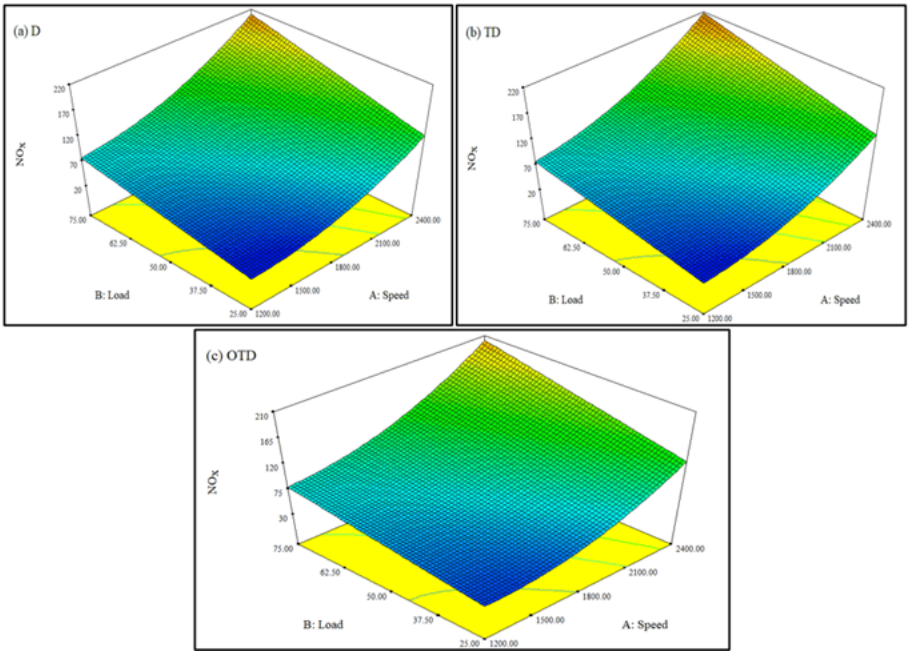

Fig. 12. Response surface plots for NO_X variation in test fuels of (a) D, (b) TD, (c) OTD, (d) APD, and (e) OAPD

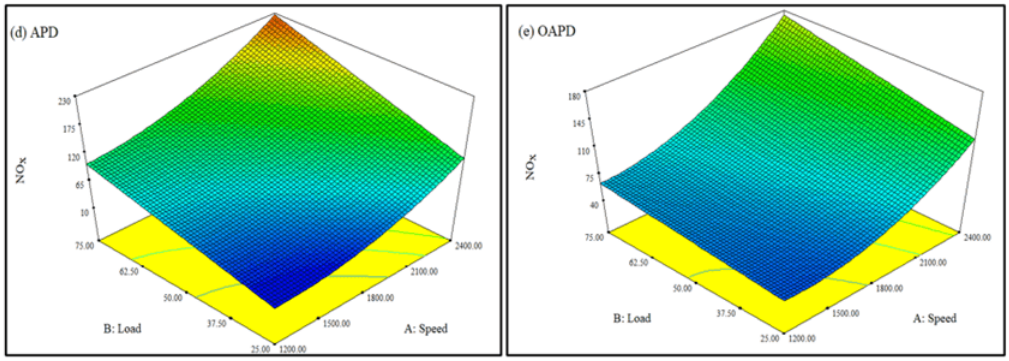

Fig. 13. Continued

4. Conclusion

The experimental investigation demonstrates that diesel blends with turpentine oil and oxygenated additives significantly influence engine performance, combustion behaviour, and emissions. All test fuels (TD, OTD, APD, and OAPD) showed improved in-cylinder pressure (ICP), with maximum values ranging from 76 bar to 79 bar compared to 75 bar for pure diesel, representing an increase of approximately 1.6%–5.3%. Similarly, the maximum heat release rate (HRR) increased from 68 J/°CA for diesel to 64–73 J/°CA for the blended fuels, reflecting a performance enhancement of up to 7.3%. Carbon dioxide (CO_2) emissions were slightly higher for the additive-diesel blends, with peak values reaching 0.8% for APD compared to 0.21% for diesel. However, carbon monoxide (CO) emissions remained low and relatively stable across all fuel types, with peak values between 0.043% and 0.046%. In contrast, nitrogen oxide (NO_x) emissions showed a significant increase, with the highest recorded value being 230 ppm for APD versus 220 ppm for diesel, marking an increase of up to 50%. The elevated NO_x levels are attributed to improved premixed combustion due to turpentine-based additives' high volatility and lower viscosity. Overall, the study confirms that while additive-diesel blends improve combustion performance, particularly under varying engine speeds and loads, they may lead to increased NO_x emissions. Proper optimization is thus essential for balancing performance gains with environmental impact.

Acknowledgement

The Faculty of Mechanical and Automotive Engineering Technology, Universiti Malaysia Pahang Al-Sultan Abdullah, Malaysia, fully supported this research.

References

Agarwal, A. K. (2007). Biofuels (alcohols and biodiesel) applications as fuels for internal combustion engines. *Progress in Energy and Combustion Science*, 33(3), 233–271.

Alenezi, R. A., Erdiwansyah, Mamat, R., Norkhizan, A. M., & Najafi, G. (2020). The effect of fusel-biodiesel blends on the emissions and performance of a single cylinder diesel engine. *Fuel*, 279, 118438. Retrieved from https://doi.org/https://doi.org/10.1016/j.fuel.2020.118438

Alenezi, R. A., Norkhizan, A. M., Mamat, R., Erdiwansyah, Najafi, G., & Mazlan, M. (2021). Investigating the contribution of carbon nanotubes and diesel-biodiesel blends to emission and combustion characteristics of diesel engine. *Fuel*, 285, 119046. Retrieved from https://doi.org/https://doi.org/10.1016/j.fuel.2020.119046

Alptekin, E., Canakci, M., Ozsezen, A. N., Turkcan, A., & Sanli, H. (2015). Using waste animal fat based biodiesels–bioethanol–diesel fuel blends in a DI diesel engine. *Fuel*, 157, 245–254.

Arpa, O., Yumrutas, R., & Alma, M. H. (2010). Effects of turpentine and gasoline-like fuel obtained from waste lubrication oil on engine performance and exhaust emission. *Energy*, 35(9), 3603–3613. Retrieved from https://doi.org/10.1016/j.energy.2010.04.050

Buyukkaya, E. (2010). Effects of biodiesel on a DI diesel engine performance, emission and combustion characteristics. *Fuel*, 89(10), 3099–3105.

Chivu, R. M., Martins, J., Popescu, F., Uzuneanu, K., Ion, I. V, Goncalves, M., … Brito, F. P. (2023). Turpentine as an additive for diesel engines: experimental study on pollutant emissions and engine performance. *Energies*, 16(13), 5150.

Elkelawy, M., Draz, A. M., Antar, A. M., & Seleem, H. E. (2025). Enhancing Diesel Generator Efficiency and Emissions with CNG and Green Hydrogen: A Sustainable Solution for Power Plants. *Pharos Engineering Science Journal*, 2(1), 47–57.

Fitriyana, D. F., Rusiyanto, R., & Maawa, W. (2025). Renewable Energy Application Research Using VOSviewer software: Bibliometric Analysis. *International Journal of Science & Advanced Technology (IJSAT)*, 1(1), 92–107.

Ganapathy, T., Gakkhar, R. P., & Murugesan, K. (2011). Influence of injection timing on performance, combustion and emission characteristics of Jatropha biodiesel engine. *Applied Energy*, 88(12),

4376–4386.
Gani, A., Saisa, S., Muhtadin, M., Bahagia, B., Erdiwansyah, E., & Lisafitri, Y. (2025). Optimisation of home grid-connected photovoltaic systems: performance analysis and energy implications. *International Journal of Engineering and Technology (IJET)*, 1(1), 63–74.
Ghazali, M. F., Rosdi, S. M., Erdiwansyah, & Mamat, R. (2025). Effect of the ethanol-fusel oil mixture on combustion stability, efficiency, and engine performance. *Results in Engineering*, 25, 104273. Retrieved from https://doi.org/https://doi.org/10.1016/j.rineng.2025.104273
Iqbal, I., Rosdi, S. M., Muhtadin, M., Erdiwansyah, E., & Faisal, M. (2025). Optimisation of combustion parameters in turbocharged engines using computational fluid dynamics modelling. *International Journal of Simulation, Optimization & Modelling*, 1(1), 63–69.
Irhamni, I., Kurnianingtyas, E., Muhtadin, M., Bahagia, B., & Yusop, A. F. (2025). Bibliometric Analysis of Renewable Energy Research Trends Using VOSviewer: Network Mapping and Topic Evolution. *International Journal of Engineering and Technology (IJET)*, 1(1), 75–82.
Jalaludin, H. A., Kamarulzaman, M. K., Sudrajad, A., Rosdi, S. M., & Erdiwansyah, E. (2025). Engine Performance Analysis Based on Speed and Throttle Through Simulation. *International Journal of Simulation, Optimization & Modelling*, 1(1), 86–93.
Karikalan, L., & Chandrasekaran, M. (2016). Influence of turpentine addition in Jatropha biodiesel on CI engine performance, combustion and exhaust emissions. *International Journal of Automotive Technology*, 17(4), 697–702.
Li, X., Liu, Q., Ma, Y., Wu, G., Yang, Z., & Fu, Q. (2024). Simulation Study on the Combustion and Emissions of a Diesel Engine with Different Oxygenated Blended Fuels. *Sustainability*, 16(2), 631.
Mohan, B., Yang, W., & kiang Chou, S. (2013). Fuel injection strategies for performance improvement and emissions reduction in compression ignition engines—A review. *Renewable and Sustainable Energy Reviews*, 28, 664–676.
Molina, S., Garcia, A., Monsalve-Serrano, J., & Villalta, D. (2021). Effects of fuel injection parameters on premixed charge compression ignition combustion and emission characteristics in a medium-duty compression ignition diesel engine. *International Journal of Engine Research*, 22(2), 443–455.
Muchlis, Y., Efriyo, A., Rosdi, S. M., & Syarif, A. (2025). Effect of Fuel Blends on In-Cylinder Pressure and Combustion Characteristics in a Compression Ignition Engine. *International Journal of Automotive & Transportation Engineering*, 1(1), 52–58.
Muhibbuddin, M., Hamidi, M. A., & Fitriyana, D. F. (2025). Bibliometric Analysis of Renewable Energy Technologies Using VOSviewer: Mapping Innovations and Applications. *International Journal of Science & Advanced Technology (IJSAT)*, 1(1), 81–91.
Muhibbuddin, M., Muchlis, Y., Syarif, A., & Jalaludin, H. A. (2025). One-dimensional Simulation of Industrial Diesel Engine. *International Journal of Automotive & Transportation Engineering*, 1(1), 10–16.
Muhtadin, M., Rosdi, S. M., Faisal, M., Erdiwansyah, E., & Mahyudin, M. (2025). Analysis of NOx, HC, and CO Emission Prediction in Internal Combustion Engines by Statistical Regression and ANOVA Methods. *International Journal of Simulation, Optimization & Modelling*, 1(1), 94–102.
Muzakki, M. I., & Putro, R. K. H. (2025). Greenhouse Gas Emission Inventory at Benowo Landfill Using IPCC Method. *International Journal of Science & Advanced Technology (IJSAT)*, 1(1), 18–28.
Nizar, M., Yana, S., Bahagia, B., & Yusop, A. F. (2025). Renewable energy integration and management: Bibliometric analysis and application of advanced technologies. *International Journal of Automotive & Transportation Engineering*, 1(1), 17–40.
Park, S. H., Youn, I. M., & Lee, C. S. (2011). Influence of ethanol blends on the combustion performance and exhaust emission characteristics of a four-cylinder diesel engine at various engine loads and injection timings. *Fuel*, 90(2), 748–755.
Rosdi, S. M., Ghazali, M. F., & Yusop, A. F. (2025). Optimization of Engine Performance and Emissions Using Ethanol-Fusel Oil Blends: A Response Surface Methodology. *International Journal of Automotive & Transportation Engineering*, 1(1), 41–51.

Rosdi, S. M. M., Erdiwansyah, Ghazali, M. F., & Mamat, R. (2025). Evaluation of engine performance and emissions using blends of gasoline, ethanol, and fusel oil. *Case Studies in Chemical and Environmental Engineering*, 11, 101065. Retrieved from https://doi.org/https://doi.org/10.1016/j.cscee.2024.101065

Rosdi, S. M., Maghfirah, G., Erdiwansyah, E., Syafrizal, S., & Muhibbuddin, M. (2025). Bibliometric Study of Renewable Energy Technology Development: Application of VOSviewer in Identifying Global Trends. *International Journal of Science & Advanced Technology (IJSAT)*, 1(1), 71–80.

Saha, D., Sinha, A., & Roy, B. (2021). Critical insights into the effects of plastic pyrolysis oil on emission and performance characteristics of CI engine. *Environmental Science and Pollution Research*, 28(33), 44598–44621.

Yumrutaş, R., Alma, M. H., Özcan, H., & Kaşka, Ö. (2008). Investigation of purified sulfate turpentine on engine performance and exhaust emission. *Fuel*, 87(2), 252–259. Retrieved from https://doi.org/10.1016/j.fuel.2007.04.019